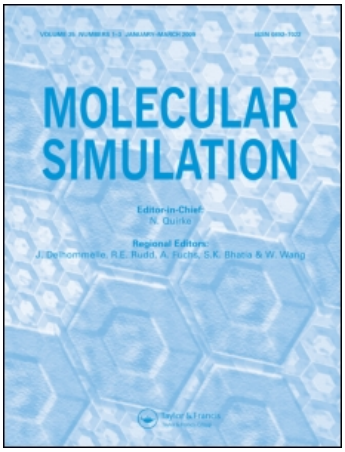

Molecular Simulation
Publication details, including instructions for authors and subscription information:
http://www.informaworld.com/smpp/title~content=t713644482

Atomic-Detail Simulation Studies of Smectic Liquid Crystals

Matthew A. Glaser[ab]; Rainer Malzbender[a]; Noel A. Clark[a]; David M. Walba[c]
[a] Department of Physics, University of Colorado, Boulder, CO [b] FOM Institute for Atomic and Molecular Physics, Amsterdam, The Netherlands [c] Department of Chemistry and Biochemistry, University of Colorado, Boulder, CO

To cite this Article Glaser, Matthew A. , Malzbender, Rainer , Clark, Noel A. and Walba, David M.(1995) 'Atomic-Detail Simulation Studies of Smectic Liquid Crystals', Molecular Simulation, 14: 4, 343 — 360
To link to this Article: DOI: 10.1080/08927029508022028
URL: http://dx.doi.org/10.1080/08927029508022028

Molecular Simulation, 1995, Vol. 14, pp. 343–360
Reprints available directly from the publisher
Photocopying permitted by license only

ATOMIC-DETAIL SIMULATION STUDIES OF SMECTIC LIQUID CRYSTALS

MATTHEW A. GLASER,[1,3] RAINER MALZBENDER,[1] NOEL A. CLARK,[1] and DAVID M. WALBA[2]

[1] *Department of Physics, University of Colorado, Boulder, CO 80309*
[2] *Department of Chemistry and Biochemistry, University of Colorado, Boulder, CO 80309*
[3] *FOM Institute for Atomic and Molecular Physics, Kruislaan 407, 1098 SJ Amsterdam, The Netherlands*

(Received September 1993, accepted January 1995)

We report on large-scale simulation studies of realistic (atomic-detail) models for smectic liquid crystals. Preliminary results obtained for the smectic *A* phase of TBBA are described in detail. Although significant obstacles must be overcome before atomic-detail simulations can yield reliable quantitative predictions of liquid crystalline properties, our results demonstrate that such simulations can provide valuable insight into the molecular basis of liquid crystalline behavior.

KEY WORDS: Smectic liquid crystals, TBBA.

1 INTRODUCTION

Thermotropic liquid crystals are of interest due to their rich polymorphism and their usefulness in display technology. Of particular interest is the relationship of liquid crystal properties and phase behavior to molecular structure. Although a number of empirical rules have been formulated, fundamental understanding of structure- property relationships in liquid crystal has been hindered by a lack of information about their microscopic structure and dynamics.

Computer simulation can provide a great deal of insight into the molecular basis of liquid crystal behavior. The study of idealized liquid crystal models has shown, for example, that purely entropic (excluded volume) effects are sufficient to produce nematic, smectic, discotic, and columnar liquid crystal phases in systems of rod-shaped molecules [1]. Real liquid crystal molecules, however, are highly structured, low-symmetry, flexible objects with complicated intra- and inter-molecular interactions. In principle, the study of more realistic models is valuable for investigating what ingredients are needed to reproduce observed liquid crystal phase behavior, and for developing intuition about liquid crystalline behavior at the microscopic level that can guide the development of microscopic theories of liquid crystal ordering. It is of interest, for example, to study the influence of molecular flexibility and deviations of molecular shape from uniaxial symmetry on liquid crystal phase diagrams, and to assess the

relative importance of entropic and energetic effects in determining liquid crystalline phase behavior. To date, however, there have been relatively few attempts to simulate liquid crystalline materials using 'realistic' (atomic-detail) molecular models [2].

There are, of course, more practical reasons for trying to improve our understanding of structure-property relationships in liquid crystals, namely their usefulness as optical switches in various applications (e.g. in display technology). For a typical application, one would like to be able to tailor the phase diagram so that a desired liquid crystal phase (e.g. nematic or smectic C^*) exists over a broad temperature range centered about room temperature. In addition, there are a number of important materials properties (dielectric anisotropy, rotational viscosities, Frank elastic constants, ferroelectric polarization density, etc.) that should be optimized for a praticular application. Computer simulation of realistic models has the potential for improving our basic understanding of structure-property relationships in liquid crystals, and thus may be a useful tool for the design of improved and/or novel materials.

In practice, computer simulations of realistic models for liquid crystalline materials face severe difficulties, the most obvious of which are related to the extreme sensitivity of liquid crystal properties and phase behavior to changes in molecular architecture, of which there are numerous examples in the literature. Generally speaking, the phase diagrams of liquid crystalline materials are determined by small free energy differences between competing phases. As a consequence, seemingly insignificant changes in molecular structure are sufficient to shift the free energy balance and dramatically alter the phase diagram. The 'delicacy' of liquid crystal ordering and phase behavior implies that highly accurate interaction potentials are required to predict structure–property relationships with any degree of realism.

Another problem confronting realistic liquid crystal simulations stems from the broad range of characteristic microscopic timescales present in liquid crystals. The fastest relevant microscopic motions are intramolecular vibrations, with periods in the range $10^{-14} - 10^{-12}$ s. Conformational transitions, reorientation of molecules around their long axes, and molecular 'rebound' due to the cage effect occur on intermediate timescales ($10^{-12} - 10^{-8}$ s). The time required for molecules to translationally diffuse one molecular diameter perpendicular to the director in nematic and smectic liquid crystals also falls in this intermediate regime, being of the order of $10^{-10} - 10^{-8}$ s. Translational diffusion of molecules by one molecular length parallel to the director takes somewhat longer ($10^{-8} - 10^{-6}$ s), whereas the corresponding process in smectics (layer-to-layer hopping) is very slow, occuring on timescales $> 10^{-5}$ s. End-for-end reorientation of molecules about their short axes is also quite slow, with a characteristic relaxation time $> 10^{-7}$ s. Although this is not an exhaustive list, it indicates the range of timescales associated with important microscopic processes in liquid crystals, which spans at least nine decades. Owing to the high density of liquid crystalline phases, it is clear that microscopic dynamical processes that involve large-scale molecular motion (e.g. end-for-end reorientation about short molecular axes) must be collective processes, involving moderate numbers of neighboring molecules. For the same reason, processes that occur in the same time regime (e.g. translational diffusion, reorientation about long molecular axes, and conformational changes) are likely to be strongly coupled.

In a molecular dynamics (MD) simulation, one must choose an integration timestep that is small compared to the fastest characteristic time in the problem, which dictates

a timestep of $\sim 10^{-5}$ s in the present case. In order to achieve adequate phase space sampling, the total duration of an MD run should be long compared to the timescale of the slowest important dynamical process in the problem (in this context, 'important' processes are those that move the system between otherwise disjoint regions of configuration space). Assuming that we can neglect the slowest processes (layer-to-layer hopping and end-for-end reorientation) in a suitably designed MD experiment, this implies that runs of $10^{-8} - 10^{-7}$ s duration may be required, which translates into $\sim 10^7 - 10^8$ MD timesteps. Although single MD runs of this length are not inconceivable, these requirements make it extremely difficult to carry out systematic studies of realistic liquid crystal models.

Finally, severe finite-size effects might be expected in simulations of small systems of liquid crystal molecules, particularly close to phase transitions, where order parameter correlation lengths become large. Available computers and current simulation techniques generally limit the linear dimension of simulated systems to $\lesssim 100$ Å, and make the systematic study of finite-size effects difficult.

If one is only interested in static properties, finite-time and finite-size effects can be somewhat alleviated by the implementation of improved sampling schemes, for instance configurational-bias Monte Carlo (CBMC) or hybrid MD-MC schemes [3]. If dynamical properties are of interest, the required investment of computer resources is necessarily larger, although multipletimestep MD methods [4] may improve the situation somewhat. Formulation of a sufficiently accurate interaction potential is in some ways the most challenging problem to overcome. In particular, methods for the accurate treatment of electrostatic interactions and induction effects in molecular simulations are still in a primitive stage of development.

Because of these challenges, atomic-detail simulation of liquid crystals is, at best, an exploratory tool at present, and it will be some time before reliable quantitative information is routinely obtainable from such simulations. Nevertheless, such simulations give access to a broad spectrum of qualitative information about the microscopic behavior of liquid crystals that is unobtainable by other means. Although the inherently large scale of such simulations inhibits systematic studies at present, even single simulations can provide valuable physical insight. This paper describes our initial attempts to model smectic liquid crystals realistically using MD simulation, and illustrates both the difficulties and the potential of such studies.

The paper is organized as follows. In section II, we describe the molecular models studied and discuss some technical details of our simulations. In section III, the results of our simulation studies are described, with an emphasis on results obtained for terephthal-bis-butylaniline (TBBA). Finally, in section IV we discuss our preliminary results and conclude with somecomments about the future prospects for simulations of this type.

2 COMPUTATIONAL METHOD

We have carried out atomic-detail MD simulations of several smectogenic liquid-crystalline materials, namely terephthal-bis-butylaniline (TBBA), p-decyloxybenzylidine-p-amino-2-methyl-butyl-cinnamate (DOBAMBC), and 4-butoxypheny-lester

4-decyloxybenzoic acid (4OP10OB). Atom-atom interactions were parametrized by the Dreiding-II empirical force field [5], which contains potential energy terms representing bonded interactions (bond stretching, bond angle bending, and torsional potential energy contributions) as well as nonbonded (van der Waals) interactions. To reduce the number of degrees of freedom and to permit the use of a relatively large integration timestep (4 fs), explicit hydrogen degrees of freedom were removed from the model (e.g. CH_2 and CH_3 groups were treated as effective atoms), and the highest-frequency intramolecular vibrations were frozen out by constraining bond lengths to their equilibrium values using the method of constraints [6]. In addition, electrostatic interactions were neglected in our simulations.

In the remainder of this section we present the details (system size, initial conditions, boundary conditions, etc.) of our simulations of TBBA. The simulations of DOBAMBC and 4OP10OB were quite similar — important differences will be pointed out where appropriate.

We simulated a system of 72 TBBA molecules with 30 effective atoms per molecule in an orthorhombic computational cell with periodic boundary conditions. The molecular centers of mass were initially arranged in two layers, each containing 36 molecules. Within each layer, the molecular centers of mass were placed on the sites of a 6×6 square lattice, and the molecular long axes were oriented parallel to the layer normal, $\hat{\mathbf{z}}$ (the procedure used to define the long axis of a molecule is described below). For liquid crystal molecules with inequivalent ends, exactly one half of the molecules were placed in each of the two possible orientations with respect to the layer normal (this initial condition imposes the $\hat{\mathbf{n}} \rightarrow -\hat{\mathbf{n}}$ symmetry exhibited by liquid crystals, where $\hat{\mathbf{n}}$ is the nematic director). Finally, the initial orientations of molecules about their long axes were randomly samples from a uniform distribution. The system was started at a relatively low density to prevent overlap of molecules. All molecules were started in the same low-energy conformation (shown in Figure 1a), and initial atomic velocities were sampled from a Maxwellian distribution, taking the effect of constraints into account using the algorithm of Ciccotti and Ryckaert [6]. Incidently, Figure 1a

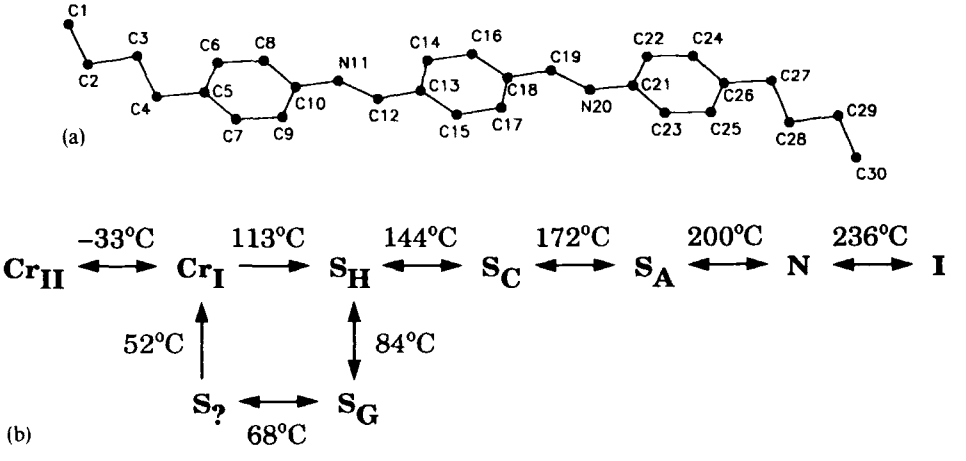

Figure 1 (a) Low energy conformation of TBBA without explicit hydrogens, showing the labelling of effective atoms. (b) Phase diagram of TBBA.

illustrates a serious shortcoming of the Dreiding II force field. This force field predicts that the potential energy of an isolated molecule of TBBA is minimized when the three phenyl rings in the core of TBBA are nearly coplanar, whereas there is abundant evidence for a substantial twist ($\sim 60°$) between adjacent rings for TBBA in its minimum-energy conformation [7]. We have observed similar problems for the other materials studied.

We carried out a 1.2 ns simulation of TBBA, which consisted of 600 ps of constant-NPT MD [8] during which the system was allowed to equilibrate (the 'thermalization run'), followed by 600 ps of microcanonical (constant-NVE) MD during which thermodynamic and statistical averages were measured (the 'main run'). L_x, L_y, and L_z (the x, y, and z dimensions of the computational cell) were allowed to vary independently during the first 600 ps of the run to accomodate a variety of possible structures, but an orthogonal cell shape was maintained. We simulated a single state point at a temperature $T = 185°C$ and pressure $P = 0$ atm, which is in the middle of the smectic A range of TBBA (see Figure 1b).

3 RESULTS

Before describing our TBBA results, we will briefly summarize the results obtained for DOBAMBC and 4OP10OB. Our simulation of 4OP10OB was identical to that of TBBA except that it was carried out at a temperature $T = 57°C$, which is in the smectic A range for this material. Our simulation results are consistent with experiment in that we observe smectic A ordering, with a smectic layer spacing that agrees well with experiment. Our simulation of DOBAMBC differed from the other simulations in that we modelled a one layer, freely suspended thin film containing 36 molecules, with free boundary conditions perpendicular to the plane of the layer and periodic boundary conditions in the plane of the layer. The simulation was carried out at a temperature $T = 110°C$, which is in the smectic C^* range for thin films. Our simulation results are consistent with experiment in that we observe smectic C ordering. Interestingly, we also observe local smectic F-like correlations (molecules are locally tilted toward their next-nearest neighbors). This is encouraging, given that DOBAMBC has a smectic F phase at lower temperatures. Our work on DOBAMBC is described elsewhere [9].

In the remainder of this section we will describe the results of our Simulation study of TBBA. We have chosen to discuss TBBA in detail here because it has proven to be more problematic than DOBAMBC or 4OP10OB, and so provides a nice illustration of the difficulties to be encountered in realistic simulations of liquid crystals.

In Figure 2 we show the time variation of L_x, L_y, L_z, the mass density ρ_m, and the potential energy per atom U/N_a during the first 600 ps of the run. All quantities (with the exception of L_z) appear to have converged by the end of the thermalization run. Particularly interesting is the pronounced asymmetry between L_x and L_y that develops between $t = 200$ ps and $t = 300$ ps, about which more will be said later. Despite the apparent attainment of equilibrium, we have good reason to believe that the system in *not* in equilibrium with respect to molecular conformations. In particular, the molecular cores remain in the conformations in which they were started for the duration of the MD run, due to the relatively large barriers (5 Kcal/mole) to dihedral rotations in the

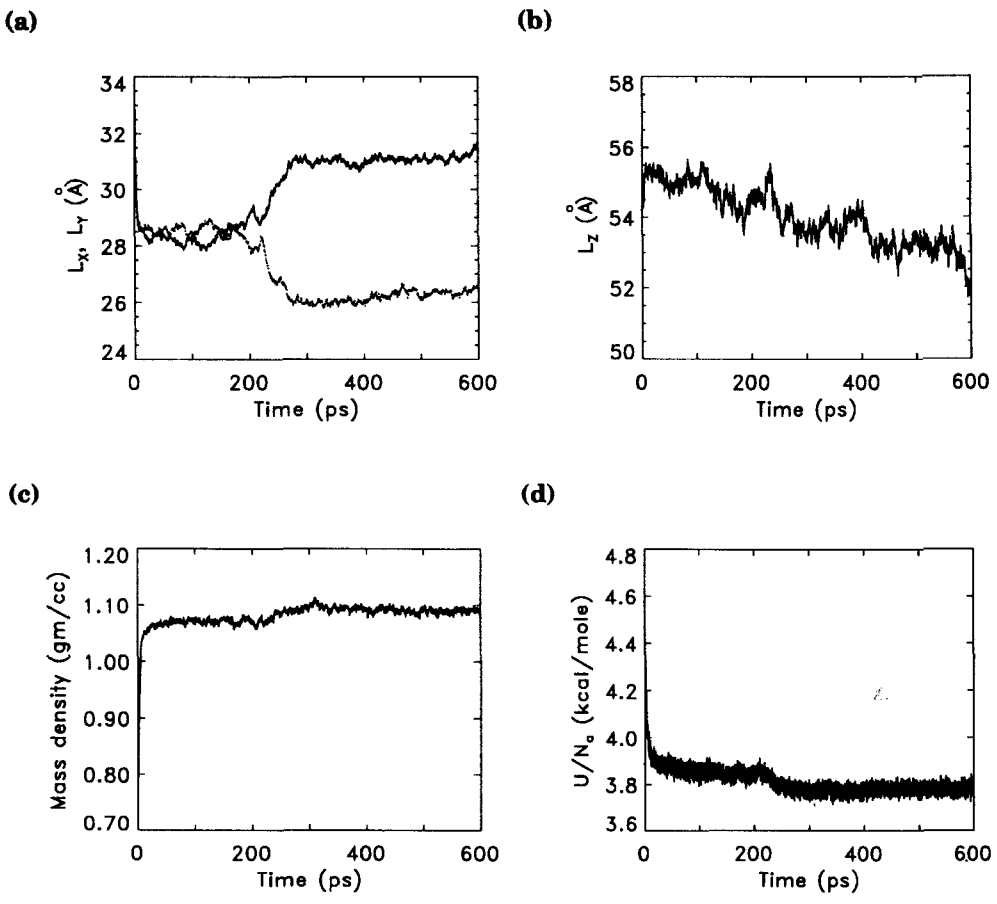

Figure 2 Time variation of various properties of the system during the thermalization run. (a) x and y dimensions of computational cell, L_x(solid line) and L_y(dotted line). (b) z dimension of computational cell, L_z. (c) Mass density, ρ_m. (d) Potential energy per atom, U/N_a.

core. A rough estimate of the chacracteristic period for conformational changes in the core is 20 ns, which is obviously much longer than the duration of the run. Because alternative core conformations are expected to be present with finite probability in thermal equilibrium, the system is probably not in conformational equilibrium.

As is apparent from Figure 2c, the system attains a rather high density of $\rho_m = 1.09$ gm/cc by the end of the thermalization run. This is significantly (13%) higher than the experimentally measured mass density at this temperature, $\rho_m = 0.96$ gm/cc [10, 11]. Such a large deviation from the experimental density is a strong indication that the simulated system possesses too high a degree of order. The density that we measure is in fact comparable to that of the crystalline phase of TBBA [10].

Figure 3 shows a 'snapshot' of the final molecular configuration from our simulation ($t = 1200$ ps). Clearly, the system still possesses well-defined smectic ordering. In fact, the time required for artificially imposed smectic order to disappear in a nematic phase

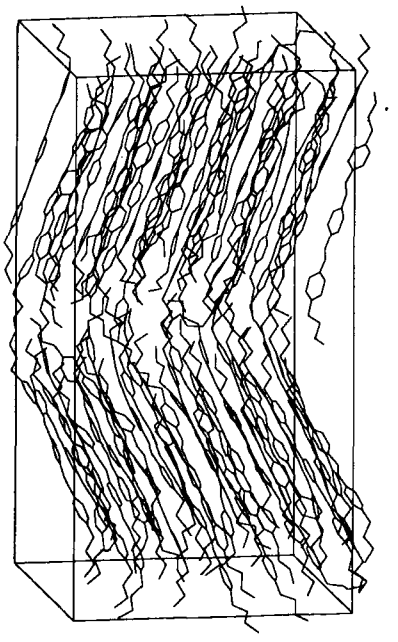

Figure 3 Instantaneous configuration of the system at $t = 1200$ ps. The molecular backbones are shown as solid lines.

is at least as large as the time required for a molecule to diffuse one molecular length (in excess of 10 ns). Given that we initially impose perfact smectic ordering, it is hardly surprising that smectic ordering remains after 1.2 ns. However, we find no evidence for a decrease in the degree of smectic ordering over the last 600 ps of the run, so it is plausible that smectic ordering is at least metastable at this temperature.

Another striking feature apparent in Figure 3 is the collective tilt of molecules away from the layer normal. Furthermore, the direction of tilt is different in the two layers, giving rise to a 'chevron' appearance. This collective tilt develops gradually during the thermalization run, a is apparent from the variation of L_z with time (Figure 2b). We believe that the 'chevroning' is an artifact of periodic boundary conditions. Because each layer is in contact with the other at two rough interfaces, it is much easier for the molecules in the two layers to tilt in opposite directions than in the same direction (the latter process requires the layers to slide over one another at atleast one interface). This tendency could perhaps be overcome by using a non-orthogonal computational cell.

To exhibit these features more clearly, we have shown a simplified representation of the final configuration in Figure 4, which shows the projection of the molecular centers of mass and long axes (molecular 'directors') into the x-z and y-z planes. Here, and in what follows, the molecular director $\hat{\mathbf{u}}$ is defined as a unit vector coincident with the minimum-moment principal axis of the molecular inertia tensor. We will also have occasion to discuss the orientation of the short molecular axes, and for that purpose define a secondary molecular director $\hat{\mathbf{v}}$ taken to coincide with the intermediate-moment principal axis of the inertia tensor. For our model of TBBA, in which the three

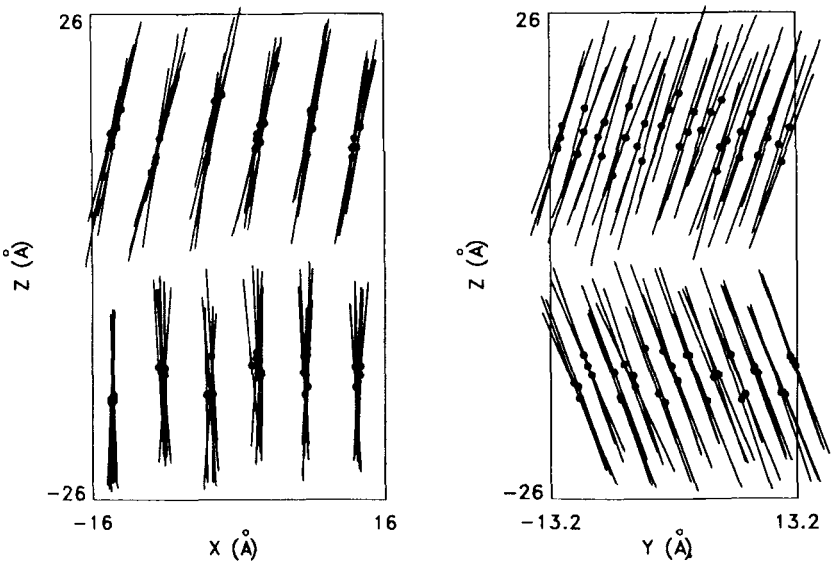

Figure 4 Simplified representation of the instantaneous configuration of the system at $t = 1200$ ps, projected into the x-z and y-z planes. The molecular centers of mass are indicated by filled circles, and the molecular directors are represented by 20 Å-long lines.

phenyl rings are nearly coplanar, $\hat{\mathbf{v}}$ lies more-or-less in the plane of the rings, and is perpendicular (by definition) to $\hat{\mathbf{u}}$.

Figure 4 shows that there are significant fluctuations of the molecular centers of mass out of the plane of the layers. To measure the size of these fluctuations, we have calculated the time-averaged center-of-mass density profile along the layer normal ($\hat{\mathbf{z}}$), which is shown in Figure 5a. The time-averaged mass density profile is also shown (Figure 5b). The peaks in the center-of-mass density profile have a FWHM of ~ 5 Å, comparable to what is measured in X-ray reflectivity experiments on freely suspended smectic thin films [12]. Because the two layers should be equivalent, the asymmetry in the density profiles of the two layers evident in Figure 5 gives an indication of the level of statistical uncertainty in our measurement.

The collective molecular tilt evident in Figure 4 persists for the duration of the main run, as evidenced by the time-averaged probability distributions of molecular tilt θ and azimuthal orientation ϕ, shown in Figure 6. The molecular tilt angle θ is defined as the angle between $\hat{\mathbf{u}}$ and the layer normal $\hat{\mathbf{z}}$, and ϕ is defined as the azimuthal orientation of $\hat{\mathbf{u}}$ in the x-y plane, measured relative to $\hat{\mathbf{x}}$. The tilt angle distribution has a well-localized peak centered at $\theta = 21.5°$. The azimuthal angle distribution exhibits two peaks, one centered at $\phi = 270.5°$, associated with the bottom layer, and one centered at $\phi = 59.5°$, associated with the top layer. The appearance of two peaks in $P(\phi)$ simply indicates that the two layers are tilted in different directions, but the magnitude of the tilt angle is very nearly the same in both layers. In Figure 6 we have also shown the θ and ϕ distributions for the molecular cores, shown as dashed lines. Evidently, the cores are more tilted on average (with a probability distribution peaked at $\theta = 24.5°$) than are

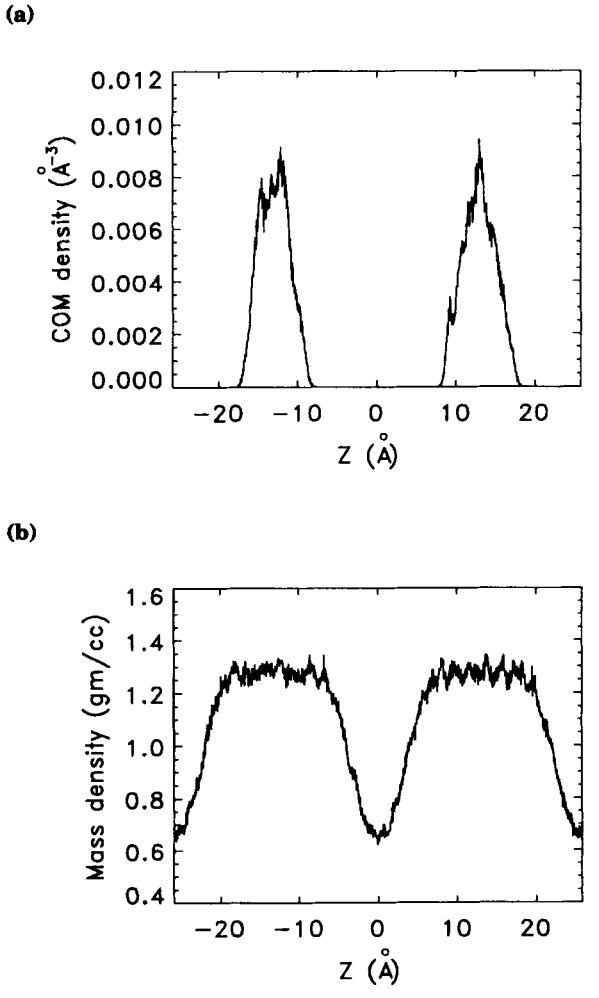

Figure 5 (a) Center-of-mass density profile and (b) mass density profile along the layer normal $\hat{z}$.

moelcules as a whole. This behavior is in accord with the zigzag model of the smectic *C* phase [13].

Similar conclusions can be drawn from an examination of the macroscopic tilt angle, as deduced from the nematic ordering tensor,

$$Q_{\alpha\beta} = \left\langle \frac{1}{N} \sum_{j=1}^{N} \left(\frac{3}{2} u_{j\alpha} u_{j\beta} - \frac{1}{2} \delta_{\alpha\beta} \right) \right\rangle, \tag{1}$$

where $\alpha, \beta = x, y, z$, the sum runs over all N molecules, and the angular braces denote an average over time. The largest eigenvalue of the ordering tensor defines the nematic order parameter S, and the corresponding eigen-vector defines the nematic director $\hat{\mathbf{n}}$ [14]. The macroscopic tilt angle Θ is defined as the angle between $\hat{\mathbf{n}}$ and the layer

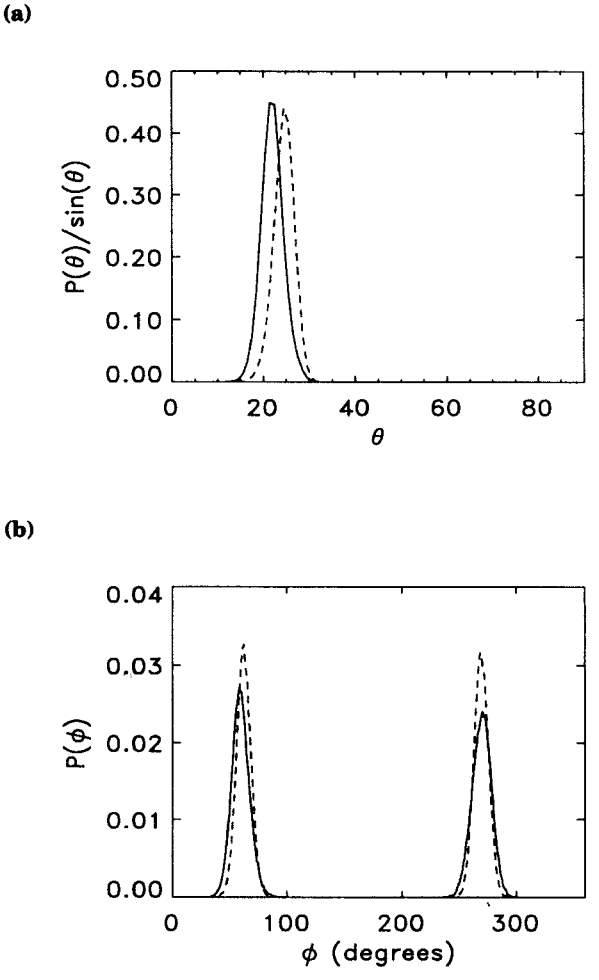

Figure 6 (a) Probability distribution of molecular tilt angles θ. (b) Probability distribution of molecular azimuthal orientations ϕ. In (a) and (b) the solid lines are the orientational distributions for molecules, while the dashed lines are the orientational distributions for molecular cores.

normal $\hat{\mathbf{z}}$ and the macroscopic azimuthal orientation Φ is defined as the azimuthal orientation of $\hat{\mathbf{n}}$ in the x-y plane, measured relative to $\hat{\mathbf{x}}$. In practice, we have calculated these quantities separately for the two layers.

We measure a high degree of overall molecular alignment, with a nematic order parameter of $S = 0.993$ for both layers. The macroscopic tilt angles for the bottom and top layers are measured to be $\Theta = 22.0°$ and $\Theta = 22.2°$, respectively, and the corresponding macroscopic azimuthal orientations are $\Phi = 269.5°$ and $\Phi = 59.5°$. The macroscopic tilt angles for the cores are larger than for the molecules as a whole: $\Theta_c = 24.9°$ for the bottom layer and $\Theta_c = 24.3°$ for the top layer. Our measured tilt angle is comparable to the saturation tilt angle for the smectic C phase of TBBA [10].

Due to the collective molecular tilt, the layer spacing measured in our simulation, $d = 25.9$ Å, is significantly smaller than that measured experimentally for the smectic A phase of TBBA at this temperature, $d = 27.7$ Å [10].

Figure 4 also reveals significant positional correlations between molecules. In particular, the projection into the x-y plane shows that the molecules are arranged in rows perpendicular to this plane. In-plane positional correlations can be seen more clearly in Figure 7, which shows projections of the molecular centers of mass into the plane of the layers (the x-y plane). The two layers are shown separately for clarity. We

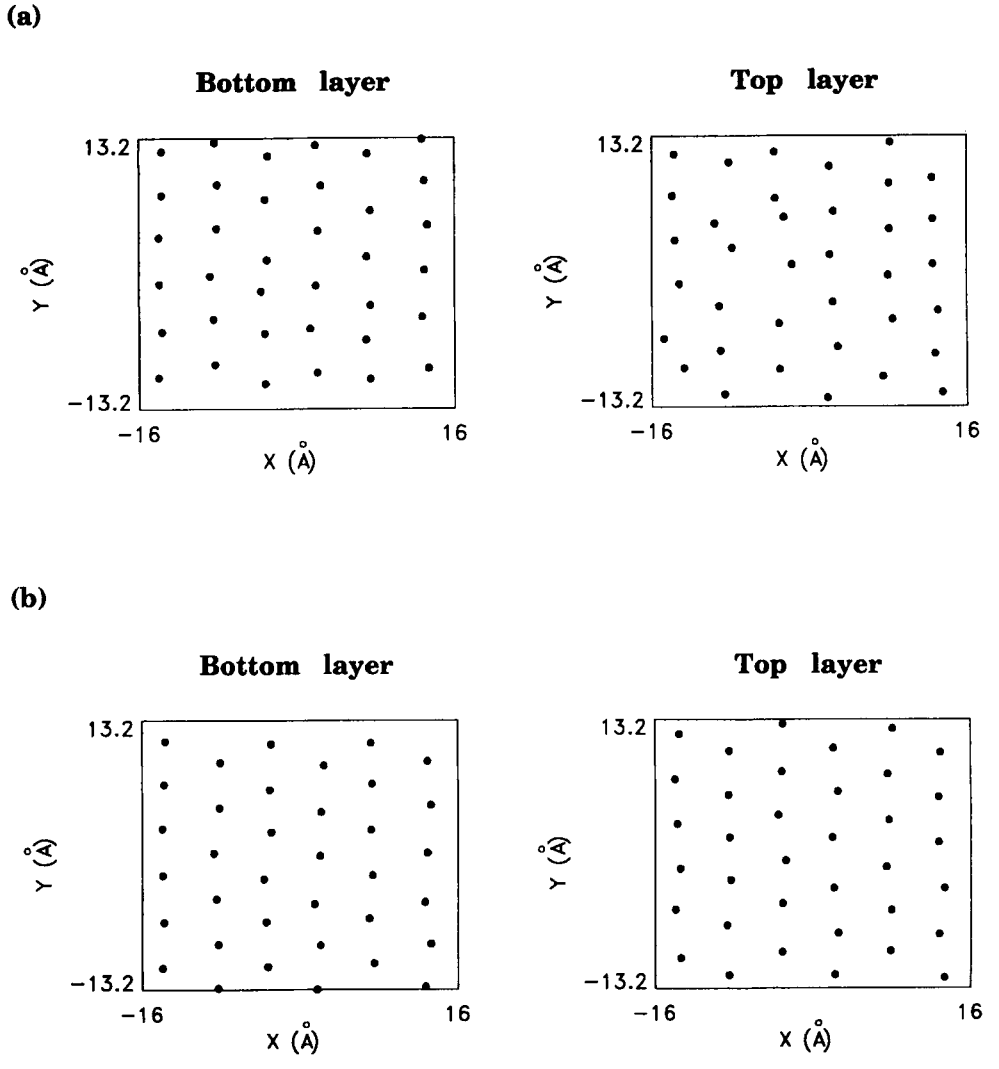

Figure 7 Projections of molecular center-of-mass positions into the layer planes for the instantaneous configuration of the system at $t = 1200$ ps. The center-of-mass positions are indicated by filled circles, and the two layers are shown separately for clarity. (a) Projection along the layer normal $\hat{z}$ (projection 1). (b) Projection along the instantaneous molecular directors (projection 2).

show two projections: in Figure 7a (projection 1), molecular centers of mass are projected into the plane of the layer along the layer normal, $\hat{z}$, while in Figure 7b (projection 2) the center of mass of each molecule is projected into the plane of the layer along its instantaneous director. Figure 7b reveals nearly perfect in-plane positional order. In this projection, the molecules are seen to form a defect-free distorted hexagonal lattice, with the orientation of the lattice the same in both layers. The projection along the layer normal (Figure 7a) appears more disordered, which implies that the out-of-plane fluctuations alluded to earlier primarily involve translational motion of molecules parallel to their long axes.

This in-plane positional ordering persists for the duration of the main run, as can be seen from the time-averaged in-plane center-of-mass density–density correlation function $g(\mathbf{R})$, shown in Figure 8. This correlation function was calculated from the in-plane center-of-mass coordinates obtained from projection 2. The formation of a distored triangular lattice is apparently responsible for the development of a pronounced asymmetry between L_x and L_y between $t = 200$ ps and $t = 300$ ps during the thermalization run (see Figure 2a).

Within each layer, the molecules are tilted more-or-less toward nearest neighbors, and the lattice constant in the tilt direction is compressed relative to the other lattice directions, yielding a distorted hexagonal arrangement. This is illustrated by Figure 9a, which shows the c-director field (the normalized projection of molecular directors $\hat{\mathbf{u}}_j$, $j = 1, N$ into the plane of the layer) for both layers. A possible reason for the distortion of the lattice is suggested by Figure 9b, in which the normalized projection of the secondary molecular directors $\hat{\mathbf{v}}_j$, $j = 1, N$ into the plane of the layer (the c2-director

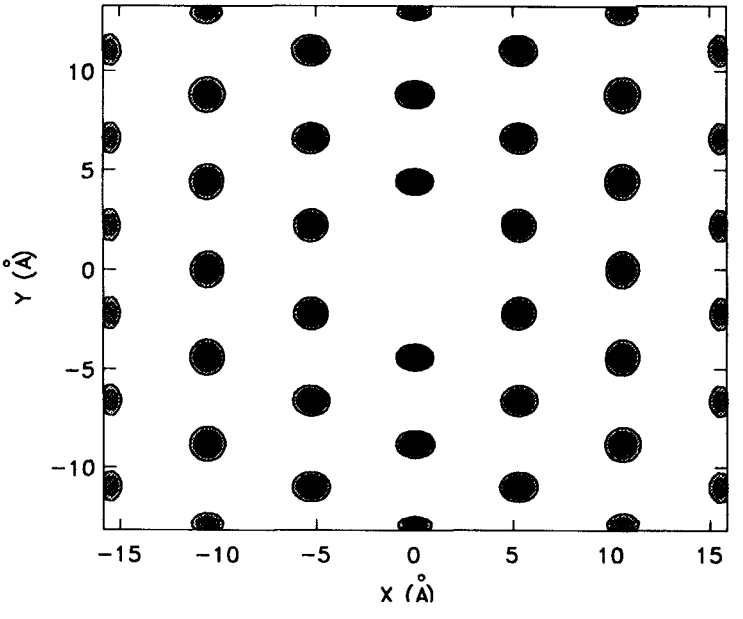

Figure 8 In-plane center-of-mass density–density correlation function $g(\mathbf{R})$, calculated from projection 2. The contour interval in 3.

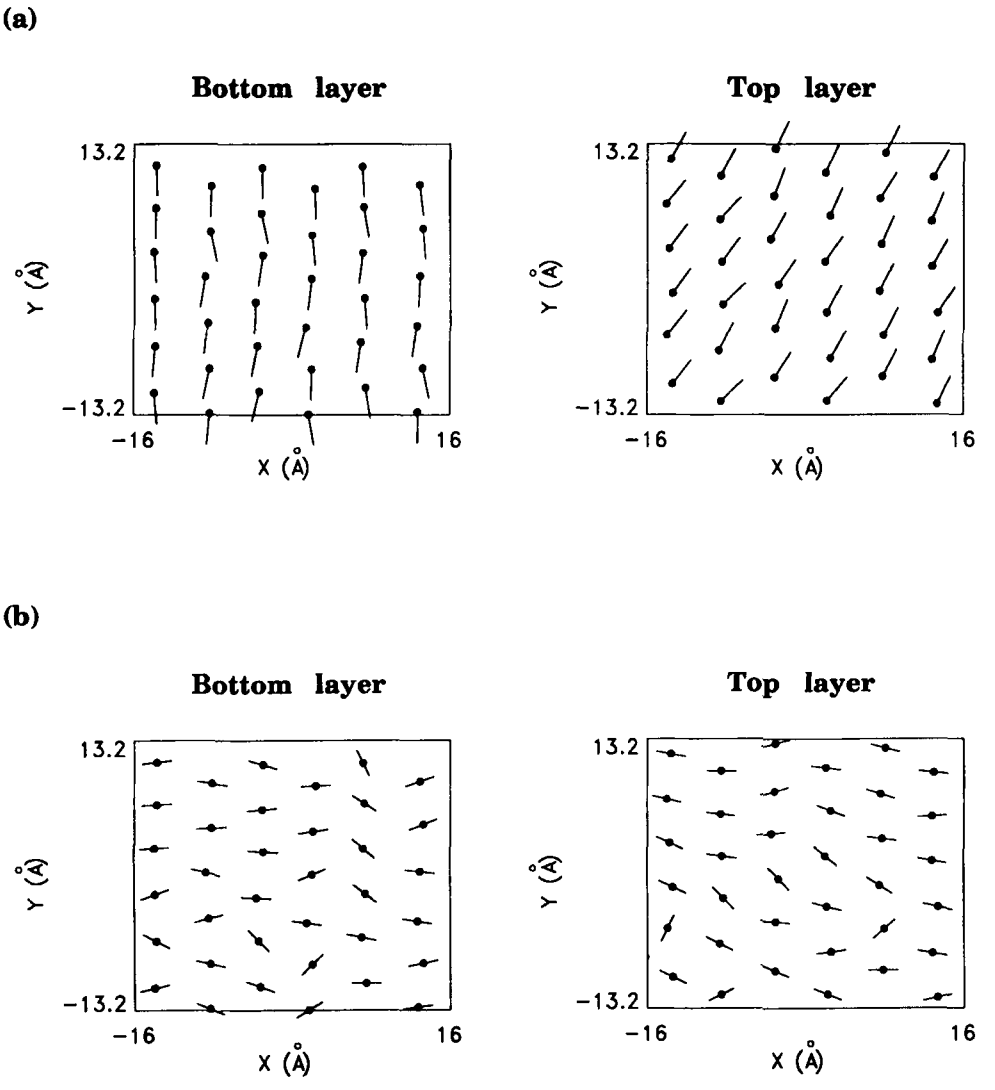

Figure 9 (a) c-director field and (b) c2-director field for the instantaneous configuration of the system $t = 1200$ ps. The in-plane center-of-mass positions (as calculated from projection 2) are indicated by filled circles, and the c- and c2-directors are represented by solid lines.

field) is shown. Figure 9b reveals a tendency for the plane of the phenyl rings (which roughly coincides with the plane defined by $\hat{\mathbf{u}}$ and $\hat{\mathbf{v}}$) to be perpendicular to the tilt plane. This tendency is further illustrated by Figure 10, which shows the distribution of angles χ between $\hat{\mathbf{v}}$ and the instantaneous molecular tilt plane. This distribution exhibits prominent peaks at 90° and 270°, indicating a strong tendency for the plane of the rings to lie perpendicular to the tilt plane. This preferential orientation of the broad dimension of the molecules perpendicular to the tilt plane may be responsible for the observed distortion of the lattice.

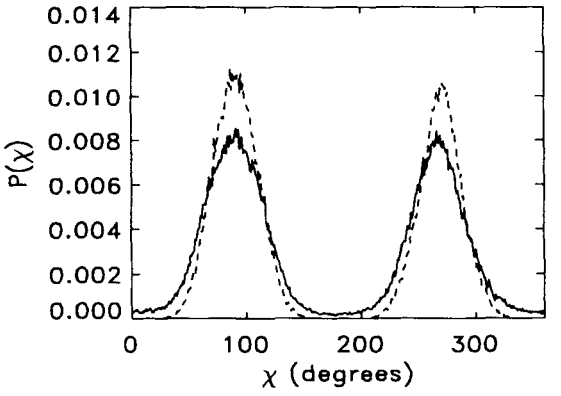

Figure 10 Orientational distribution of the molecular short axis with respect to the instantaneous molecules tilt plane. The solid line is the orientational distribution for molecules, while the dashed line is the orientational distribution for molecular cores.

To study the in-layer ordering in more detail, we have calculated the in-plane sixfold bond orientational correlation function. The general formula for an order-parameter correlation function is

$$g'_O(\mathbf{R}) = \langle O(\mathbf{0})O(\mathbf{R})\rangle, \tag{2}$$

where the order parameter density $O(\mathbf{R})$ is defined by

$$O(\mathbf{R}) = \sum_{j=1}^{N} O_j \delta(\mathbf{R} - \mathbf{R}_j). \tag{3}$$

The sum ranges over all N molecules, O_j is a microscopic order parameter associated with molecule j, and $\mathbf{R}_j$ is the in-plane position of molecule j as calculated from projection 2. In the case of sixfold bond orientational order, the microscopic order parameter is defined as

$$O_j = \frac{1}{n_j} \sum_{k=1}^{n_j} e^{i6\gamma_{jk}}, \tag{4}$$

where the sum runs over the n_j nearest neightbors of molecule j [15], and γ_{jk} is the orientation of the 'bond' between molecules j and k with respect to an arbitrary axis (in this case the x axis). In practice, we measured only the angle-averaged sixfold bond orientational correlation function,

$$\acute{g}_6(R) = \frac{1}{2\pi} \int_0^{2\pi} \acute{g}_6(R, \Theta) d\Theta, \tag{5}$$

where $R = |\mathbf{R}|$, and Θ is the polar orientation of $\mathbf{R}$ in the plane of the layer. Translational correlations were removed from $\acute{g}_6(R)$ by dividing it by the angle-averaged pair correlation function $g(R)$,

$$g_6(R) = \acute{g}_6(R)/g(R). \tag{6}$$

$g(R)$ and $g_6(R)$ are shown in Figure 11. $g_6(R)$ approaches a nonzero constant for large R, which suggests that the system possesses long-range bond orientational order.

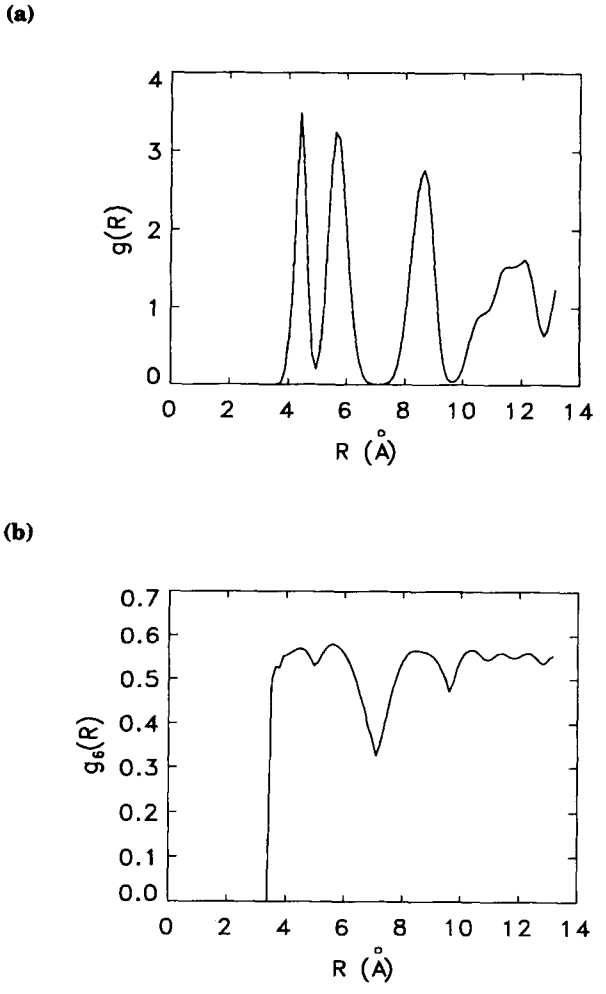

Figure 11 Angle-averaged in-plane correlation functions. (a) Pair distribution function $g(R)$. (b) Sixfold bond-orientational correlation function $g_6(R)$.

Similarly, $g(R)$ reveals extended positional correlations, but it is impossible to say whether the in-plane positional correlations are truly long-ranged or of large but finite range.

Finally, we can examine the degree of conformational disorder by measuring the dihedral angle distributions for various internal rotations within the molecule. As mentioned earlier, the cores behave almost rigidly, due to the large barriers to internal rotation about bonds in the core. The tails, on the other hand, are somewhat flexible, as illustrated by Figure 12, in which the dihedral angle distributions for torsions α (involving atoms 7, 5, 4, and 3), β (atoms 5, 4, 3, and 2), and γ (atoms 4, 3, 2, and 1) are displayed (owing to the end-for-end symmetry of the molecule, the dihedral distributions for the other tail are nearly identical to those shown here). In our convention the trans conformation corresponds to a dihedral angle of $\pm 180°$. Figure 12a shows that the

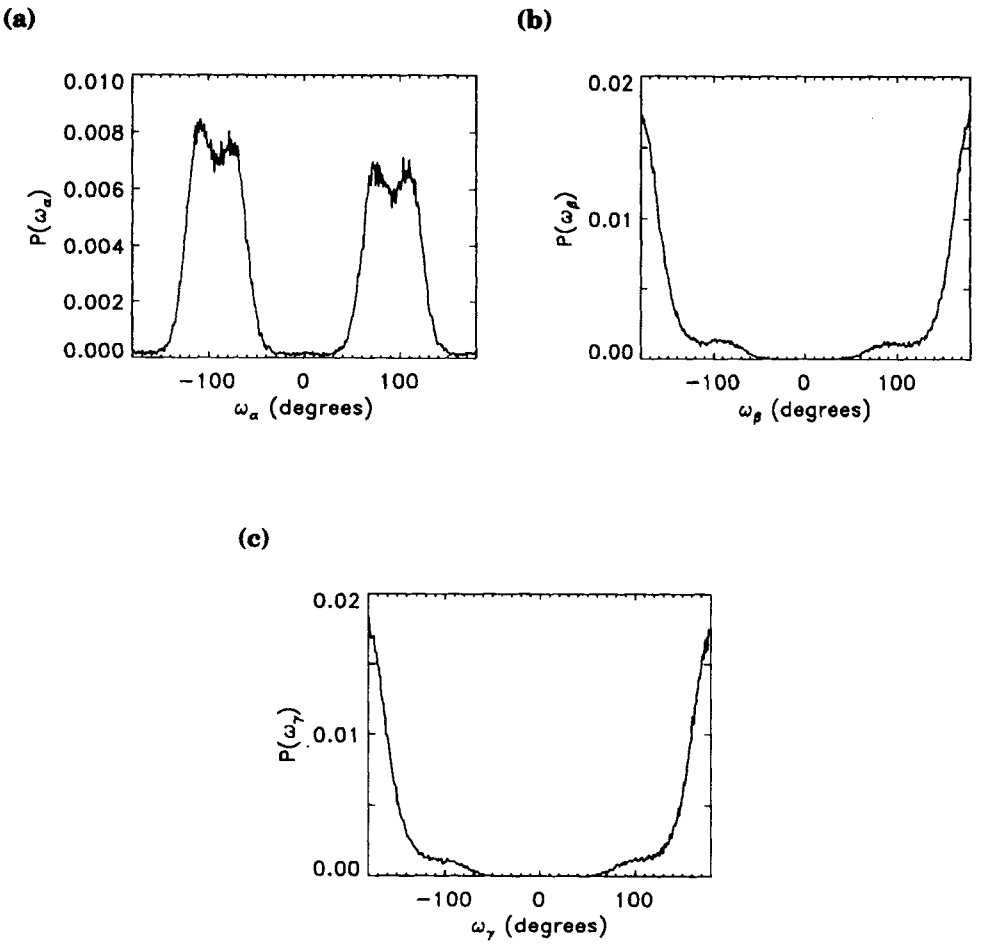

Figure 12 Orientational distributions for dihedral rotations about the (a) first, (b) second, and (c) third bonds in the alkyl tail of TBBA.

plane defined by the first two bonds in the tail tends to be nearly perpendicular to the plane of the ring to which it is attached, with nearly equal populations around $\omega_\alpha = -90°$ and $\omega_\beta = +90°$. In addition, there is a finite population of gauche bends around the second and third bonds in the tail, as can be seen from Figure 12b and 12c.

4 DISCUSSION AND CONCLUSIONS

At first glance, our attempt to simulate the smectic *A* phase of TBBA appears to be a spectacular failure. Instead of the orthogonal smectic *A* phase, we observe a *tilted* smectic phase. What is more, the high degree of in-plane ordering reveals the observed phase to be a higher-order smectic, with long-range bond orientational order, andwith molecules tilted toward nearest neighbors. It is not possible to make a definte statement

about the in-plane translational order. Clearly, the system is not perfectly ordered — out-of-layer translation of molecules along their long axes appears to be an inportant fluctuation mode, and molecules exhibit hindered rotation about their long axes as well as some conformational disorder. On this basis we can tentatively identify the phase we observe as a smectic *I* (hexatic) or smectic *J* (crystalline) phase. Unfortunately, neither the smectic *I* or smectic *J* phases appear in the phase diagram of TBBA. TBBA does have tilted smectic phases, namely the smectic *C*, *H*, and *G* phases, but the higher-order smectics that are observed (smectic *G* and *H*) are ones in which the molecules are tilted toward next-nearest neighbors rather than nearest neighbors.

Our result for TBBA, although rather discouraging, do give some indication of the range of microscopic structural and dynamical information that is, in principle, accessible in simulations of this type. In light of the technical obstacles facing atomic-detail simulations of liquid crystals, it will likely be some time before they can yield reliable quantitative predictions. Nevertheless, we believe that this method can provide valuable insight into the molecular basis of liquid crystalline behavior. For example, our simulation study of TBBA suggests that electrostatic interactions are not required to produce tilted smectics. Our observation of a smectic *C* phase in simulations of DOBAMBC thin films (also without electrostatics) [9] lends further support to this conclusion. These findings are at variance with microscopic models of the smectic *C* phase that rely on electrostatic interactions to produce molecular tilt [16], and are more consistent with the zigzag model of the smectic *C* phase [13], in which the zigzag shape of molecules results in a 'freeze-out' of the rotation of molecules around their long axes, which in turn induces a molecular tilt. Although the small sample size in our simulation precludes any definitive statement about the behavior of bulk systems, we feel that out results are suggestive.

The foregoing discussion suggests a number of possible causes for our failure to reproduce the correct phase behavior in TBBA: (1) the empirical force field used in this study constrains the phenyl rings in the core of TBBA to be nearly coplanar, whereas there is compelling evidence from a variety of sources for a nonplanar conformation of the core; (2) our simulation does not effectively sample alternative core conformations; (3) electrostatic interactions and induction effects are not included in our simulations; (4) finite-size effects could lead to too high a degree of ordering.

It is possible to improve on our current methodology in several ways. More accurate (albeit more complex) empirical force fields have been developed (e.g. MM2 and MM3 [17]). We plan to incorporate a more accurate empirical force field into our simulations in the near future. More effective sampling of molecular conformations will probably require the use of special MC schemes (e.g. configurational-bias Monte Carlo or hybrid MC-MD algorithms [3]). Work on such improved sampling algorithms is currently under way. The proper treatment of electrostatic interactions and induction effects is more problematic. It is possible at present to treat electrostatic interactions in an approximate way, but much work remains to be done in this area. Finally, the analysis of finite-size effects is contingent upon the development of more efficient simulation methods and the availability of improved computer hardware.

Clearly, the realistic simulation of liquid crystalline systems poses significant challenges. However, the potential of this approach for revealing new physics and guiding materials development make it a challenge well worth taking up.

Acknowledgement

This work was supported by the National Science Foundation Materials Synthesis and Processing Program Grant DMR-9202312 and by the National Science Foundation Materials Research Group Grant DMR-9224168.

References

[1] D. Frenkel, "Statistical Mechanics of Liquid Crystals," in Liquids, Freezing, and the Glass Transition, edited by J.P. Hansen, D. Levesque, and J. Zinn-Justin (North-Holland, Amsterdam, 1991).

[2] M.R. Wilson and M.P. Allen. "Structure of trans-4-(trans-4-*n*-pentylcyclohexyl)cyclohexylcarbonitrile (CCH5) in the isotropic and nematic phases: a computer simulation study," *Liq. Cryst.* **12**, 157 (1992); M.R. Wilson and M.P. Allen. "Computer Simulations of Mesogenic Molecules Using Realistic Atom–Atom Potentials," *Mol. Cryst. Liq. Cryst.* **198**, 465 (1991); I. Ono and S. Kondo. "Orientational Ordering and Molecular Motion of 4'-pentyloxy-4-cyanobiphenyl (5OCB) by Molecular Dynamics Simulation," *Mol. Cryst. Liq. Cryst. Lett.* **8**, 69 (1991); B. Jung and B.L. Schürmann. "Molecular Dynamics Simulations of Phenyl-4-(4-benzoyloxy)benzoyloxybenzoate in the Crystalline and Nematic Phase," *Mol. Cryst. Liq. Cryst.* **185**, 141 (1990); S.J. Picken, W.F. van Gunsteren, P. Th. van Duijnen and W.H. de Jeu. "A molecular dynamics study of the nematic phase of 4-*n*-pentyl-4'-cyanobiphenyl," *Liq. Cryst.* **6**, 357 (1989); A.V. Komolkin, Yu.V. Molchanov, and P.P. Yakutseni. "Computer simulation of a real liquid crystal," *Liq. Cryst.* **6**, 39 (1989).

[3] D. Frenkel. "Advanced Monte Carlo Techniques," in Computer Simulation in Chemical Physics, edited by M.P. Allen and D.J. Tildesley (Kluwer Academic, Dordrecht, 1993).

[4] M. Tuckerman, B.J. Berne, and G.J. Martyna. "Reversible multiple time scale molecular dynamics," *J. Chem. Phys.* **97**, 1990 (1992).

[5] S.L. Mayo, B.D. Olafson, and W.A. Goddard III. " DREIDING: A Generic Force Field for Molecular Simulations," *J. Phys. Chem.* **94**, 8897 (1990).

[6] G. Ciccotti and J.P. Ryckaert. "Molecular Dynamics Simulation of Rigid Molecules," *Comp. Phys. Rep.* **4**, 345 (1986).

[7] H. Perrin and J. Berges. "Theoretical conformational study of the TBBA molecule," *J. Physique Lett.* **43**, L531 (1982).

[8] H.J.C. Berendsen, J.P.M. Postma, W.F. van Gunsteren, A. Dinola, and J.R. Haak. "Molecular dynamics with coupling to an external bath," *J. Chem. Phys.* **81**, 3684 (1984).

[9] M.A. Glaser, R. Malzbender, N.A. Clark, and D.M. Walba. "Atomic detail simulation studies of tilted smecties," *J. Phys.: Condens. Matter.* **6**, A261 (1994).

[10] D. Guillon and A. Skoulios. "Polymorphisme smectique du paraben-zylidène-di-n, butyl-4-aniline (TBBA)," *J. Physique* **38**, 79 (1977).

[11] N.V.S. Rao and V.G.K.M. Pisipati. "Specific Volume Studies in Nematic, Smectic-A and Smectic-C Phases of TBBA," *Mol. Cryst. Liq. Cryst.* **104**, 301 (1984).

[12] D.J. Tweet, R. Holyst, B.D. Swanson, H. Stragier, and L.B. Sorenson. "X-Ray Determination of the Molecular Tilt and Layer Fluctuation Profiles of Freely Suspended Liquid-Crystal Films," *Phys. Rev. Lett.* **65**, 2157 (1990).

[13] R. Bartolino, J. Doucet, and G. Durand. "Molecular Tilt in the Smectic C Phase: A Zigzag Model," *Ann. Phys.* **3**, 389 (1978).

[14] Alternatively, one could take minus twice the middle eigenvalue of the ordering tensor as the nematic order parameter S (see Eppenga and Frenkel, "Monte Carlo study of the isotropic and nematic phases of infinitely thin hard platelets," *Mol. Phys.* **52**, 1303 (1984)). In practice, we find good agreement between the two definitions of S.

[15] Our definition of nearest neighbors is based on the Voronoi construction, which assigns a Voronoi cell to each molecule, defined (in two dimensions) as the region of the plane that is closer to a given molecule than to any other molecule. Any pair of molecules whose Voronoi cells share a side are taken to be nearest neighbors.

[16] See, for example, G. Vertogen and W.H. de Jeu. Thermotropic Liquid Crystals, Fundamentals (Springer-Verlag, Berlin, 1988).

[17] See N.L. Allinger, Z.S.Z. Zhu, and K. Chen. "Molecular Mechanics (MM3) Studies of Carboxylic Acids and Esters," *J. Am. Chem. Soc.* **114**, 6120 (1992), and references therein.